Vol. 23, n.°1, pp. 25-38, 2024
Revista UIS Ingenierías
https://revistas.uis.edu.co/index.php/revistauisingenierias

Potential Use of Fryze's Approach-Based Power Theories in Waveform Distortion Contribution Assessment

Uso potencial de las Teorias de Potencia basadas en el enfoque de Fryze para evaluar contribución a la distorsión de forma de onda

Camilo Garzón [1a], Ana María Blanco [2a], Andrés Pavas [1b], Jan Meyer [2b]

[1] Universidad Nacional de Colombia, Colombia. Orcid: 000-0002-1658-179X [a], 0000-0002-0971-0725 [b]. Emails: cagarzon@unal.edu.co [a], fapavasm@unal.edu.co [b].
[2] TUD Dresden University of Technology, Alemania. Orcid: 0000-0002-7465-5750 [a], 0000-0002-6884-5101 [b]. Emails: ana.blanco@tu-dresden.de [a], jan.meyer@tu-dresden.de [b].

Received: 12 July 2023. Accepted: 15 October 2023. Final version: 4 January 2024.

Abstract

This paper explores the potential of some remarkable power theories derived from Fryze's approach to assessing waveform distortion contributions. The analysis is limited to a simplified system composed of one load and one voltage source connected by a point of common coupling. Finally, some keys to assess are proposed for two types of systems: strong networks (traditional distribution systems) and weak networks (islanded microgrids).

Keywords: Power Theories; Responsibilities Assessment; Power Quality; Disturbances.

Resumen

Este artículo explora el potencial de algunas teorías de potencia notables derivadas del enfoque de Fryze para evaluar las contribuciones a la distorsión de formas de onda. El análisis se limita a un sistema simplificado compuesto por una carga y una fuente de voltaje conectadas por un punto de acople común. Finalmente, se proponen algunas claves para evaluar dos tipos de sistemas: redes fuertes (sistemas de distribución tradicionales) y redes débiles (microrredes aisladas).

Palabras clave: teorías de potencia; asignación de responsabilidades; calidad de potencia; perturbaciones.

1. Introduction

Power quality disturbances have been widely studied, and particularly, waveform distortion has been the focus of many papers given the well-known effects of such disturbance over the network [1]. Usually, the frequency domain approach is used to assess, for example, emission limits in terms of harmonics components [2], [1], or responsibility assignment [2], [3], [4]. Nevertheless, more information about the system is needed for this analysis, like the harmonic network impedance or multipoint measurements.

ISSN Online: 2145 - 8456

How to cite: C. Garzón, A. M. Blanco, A. Pavas, J. Meyer, "Potential Use of Fryze's Approach-Based Power Theories in Waveform Distortion Contribution Assessment," *Rev. UIS Ing.*, vol. 23, no. 1, pp. 25-38, 2024, doi: https://doi.org/10.18273/revuin.v23n1-2024003

The waveform distortion contribution method quantifies the amount of distortion injected by each customer connected to the point of Common Coupling (PCC). Although a PCC can connect many feeders, this problem is usually reduced to two agents, the load and network sides. The simplification is helpful in practical scenarios where knowing the impact of the load side is desirable. Still, more than one measurement point is required if assessing more than one load. In this way, there are a lot of methods to determine the waveform distortion contribution or simply contribution throughout this text. Many of these are based on the Thevenin or Norton equivalent; some remarkable methods are summarized and analyzed in [5]. Nevertheless, this is still an open issue, given that there is no agreement about the reliability of the results, practical application, and plausible physical interpretation of the methods.

This paper approaches the problem of waveform distortion contribution from Fryze's power theory framework. The aim is to explore the potential of the more remarkable power theories derived from Fryze's proposal to assess responsibilities in a reduced system composed of a PCC and two agents, the load and the network. In this way, in section II, the mathematical definitions of voltage, current, active power, and nonactive power are presented using the Fourier series approach. These definitions are widely accepted and are the basis for developing this paper.

Section III presents the power theories from a mathematical point of view, identifying their advantages, some limitations, and the main differences between them. In section IV, a study case was designed and implemented in the laboratory to test the power theories under different types of loads and voltage sources. Finally, the test results are analyzed and discussed in section V.

2. Remarkable Power Theories and Power Definitions

According to [6], three schools currently dominate power theory definitions: Constantin I. Budeanu's school, Stanislaw Frize's school [7], [8], and the Pointing Vector based power theory (IEEE Std. 1459 recommendation) [6], [9]. However, Budeanu's approach has been strongly criticized and abandoned by many researchers [10], [11]. Four power theories are currently the most accepted but widely discussed by the remaining two schools. One of them is the already mentioned IEEE Std. 1459 [9]. The other three are based on Fryze's work, namely, FBD power theory [12], [13], Conservative Power Theory [14], [15], and Current's Physical Components power theory [16], [17]. They define reactive power to obtain and perform different orthogonal decomposition over the non-active powers. According to [17], a power theory has to fulfill the following requirements:

1. *A n explanation and physical interpretation of power phenomena that accompany energy delivery*
2. *A definition of power quantities which describe energy flow and its utilization, as well as can specify power ratings of the power equipment*
3. *Fundamentals for energy accounts between energy producers and customers*
4. *Fundamentals for studies on the effectiveness of energy delivery*
5. *Fundamentals for design and control of equipment for power factor improvement*
6. *Fundamentals for design and control of equipment for loading and supply quality improvement*

Indeed, the four theories agree on the first, the first part of the second, and the third requirement, understanding this as the formulation for power and energy calculations. The rest of the conditions are unclear to the authors, given that the fundamentals for studies and design, understanding "fundamentals" as the inputs, more than a requirement, is a natural result. In this way, it is possible to say that any power theory accomplishes the last three requirements.

Considering the agreement between power theories already commented on, it is widely accepted that active power is a physical definition representing the energy exchange rate in a system. Particularly in electrical systems, such power is defined as (1):

$$P = \frac{1}{T}\int_{\tau}^{\tau+T} i(t)u(t)dt = \frac{1}{T}\int_{\tau}^{\tau+T} p(t)dt \qquad (1)$$

Where $p(t)$ is the instantaneous power, T is the period, and $u(t)$ is the voltage, which can be defined for non-sinusoidal conditions as:

$$u(t) = U_0 + \sqrt{2}U_1 \sin(\omega_1 t + \alpha_1) + \sqrt{2}\sum_{h=2}^{H} U_h \sin(h\omega_1 t + \alpha_h) \qquad (2)$$

Where the first term is the DC component, this term must be considered only if the DC level is observed in the measurement. The second term is the fundamental frequency component, and the third term could be considered as the voltage distortion reflected on the PCC.

Finally, the current $i(t)$ can be expressed in the same manner as:

$$i(t) = I_0 + \sqrt{2}I_1 \sin(\omega_1 t + \beta_1) + \sqrt{2}\sum_{h=2}^{H} I_h \sin(h\omega_1 t + \beta_h) \quad (3)$$

According to 1, the components $u_h(t)$ that match with the components $ih(t)$ and also are in phase shape the active power P. This implies that the voltage distortion of the network is reflected in the power P. In other words, voltage distortion is reflected in the active power. All the components $i_h(t)$ that match with the components $u_h(t)$ can be called active harmonic components, given that such components are involved in the energy exchange.

It is worth clarifying that each harmonic component h in the equations 2 and 3 is a phasor quantity composed by a magnitude U_h and a phase angle α_h for voltage case. Otherwise, the rms values of $u(t)$ and $i(t)$ can be calculated as:

$$U = \sqrt{\frac{1}{T}\int_{\tau}^{\tau+T} u^2(t)dt} \quad (4)$$

$$I = \sqrt{\frac{1}{T}\int_{\tau}^{\tau+T} i^2(t)dt} \quad (5)$$

Then, the apparent power, representing the maximum power rating of the equipment, can be defined as:

$$S = UI \quad (6)$$

From definitions 1 and 6, Non-active power is defined as:

$$N = \sqrt{S^2 - P^2} \quad (7)$$

Active power exchange is a desirable condition in the power system. As it was shown in [11] that active harmonic components flow in the same direction as the fundamental harmonic component, feeding the loads even under non-sinusoidal conditions.

Otherwise, non-active power contains all the information related to no-energy exchange; in other words, non-active power is related to all power quality disturbances except active harmonic powers. However, each power theory's treatment of this amount can be slightly different. This means that the first three requirements mentioned above are satisfied by each power theory in different ways; in fact, the results of each approach could change. However, all the results obtained from each method can be helpful depending on the context and the objectives of the analysis in progress. At this point, it is worth mentioning that all power quality disturbances are not necessarily undesirable; some of them, like fundamental reactive power, are inherent to some equipment in the network and even necessary for the normal functioning of such equipment [18].

3. Power Theories Based on Fryze's Approach

This paper is focused only on Fryze's approach. This school started with a time-domain theory proposed by S. Fryze [7], extended to multiconductor systems by F. Buchholz [8], and generalized for nonsinusoidal systems by M. Depenbrock [12] (FBD power theory) and L. Czarnecki [16] (Current's Physical Components power theory). P. Tenti developed an additional improvement to Fryze's approach [14] and aimed to describe nonactive powers in terms of conservative variables (Conservative power theory). In Fryze's approach, it is assumed the existence of a fictitious equivalent conductance (Eq 8):

$$G = \frac{P}{U^2} \quad (8)$$

This quantity is suitable for modeling the active power flow from the voltage source to the loads, as shown in Fig. 1. However, note that G not only represents the demanded fundamental active power, but it also represents the active harmonic power produced by the presence of voltage distortion, then, the quantity:

$$i_a(t) = Gu(t) = \frac{\langle u(t), i(t)\rangle}{UI^2}u(t) \quad (9)$$

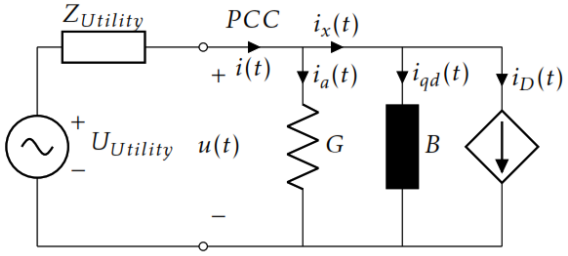

Figure 1. FBD Power Theory. Source: Own elaboration.

Known as active current, it forms along with the *PCC* voltage, the active power of the load. Since active power represents the energy exchange, all active harmonic components flow in the same direction as the fundamental since energy generation is only possible in the power source [13]. It means that the effects of voltage distortion in traditional distribution systems are reflected

in the active current component. Thus, the following statements remain valid for any distribution system:

- Active current, as defined in 9, can only flow from the power sources to the loads, given that loads cannot generate energy.
- It is possible that power sources share active current components. However, the active fundamental component always flows from power sources to loads.

On the other hand, a decomposition over *non-active* current $i_x(t)$ is performed, splitting it into two orthogonal components represented in Fig. 2 by the susceptance B and the current source D. The definitions of B and D differ for each power theory mentioned; these variables and the associated powers can be interpreted differently. The equations of FBD power theory (FBD), Conservative power theory (CPT), and Current's Physical Components power theory (CPC) will be described below.

3.1. FBD Power Theory (FBD)

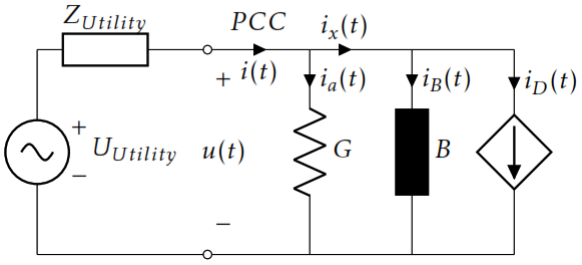

Figure 2. Extended Fryze's approach. Source: Own elaboration.

In this power theory (Fig. 1 displaced voltage $u_d(t)$ is defined as the voltage of the source displaced a quarter of period ($u_d(t)=u(T\text{-}T/4)$). This definition allows to calculate the *displaced power*:

$$Q_d = \frac{1}{T}\int_{\tau}^{\tau+T} i_x(t)u_d(t)dt \qquad (10)$$

Where the nonactive current is calculated as $i_x(t) = i(t)i_a(t)$. Then, it is possible to define a *displaced current* $i_{qd}(t)$, associated with phase displacement, as:

$$i_{qd}(t) = Bu_d(t) = \frac{Q_d}{U^2}u_d(t) \qquad (11)$$

Note that the voltage used as a reference for i_{qd} calculation has the same waveform of $u(t)$, which means that displaced current contains information related to phase displacement even in nonfundamental frequencies. Thus, voltage distortion is also reflected in the displaced current. Finally, the *Distorted current* $i_D(t)$ is associated with waveform distortion unrelated to active and displaced components.

$$i_D(t) = i(t) - i_a(t) - i_{qd}(t) \qquad (12)$$

In this paper, the phase unbalance is neglected. However, a detailed description of the FBD decomposition process for single-phase and multi-phase systems is presented in [19].

3.2. Conservative Power Theory (CPT)

This theory resembles FBD (Fig. 3). The main difference is the voltage reference to decompose $i_x(t)$. In this way, a quantity called *unbiased voltage* is defined as:

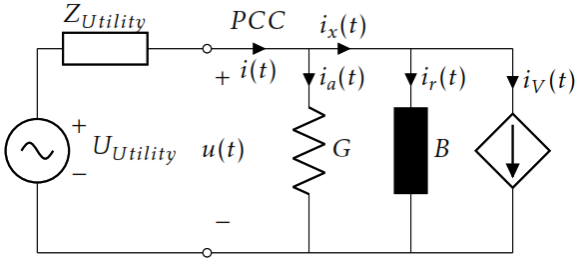

Figure 3. Conservative power theory approach. Source: Own elaboration.

$$\hat{u}(t) = \int_0^t u(\tau)(d\tau) - \frac{1}{T}\int_0^T u(t)dt \qquad (13)$$

Where the mean value of $u(t)$ is used as an unbiased estimator, note that the second term of 13 is zero without the DC level. On the other hand, the first term displaces the voltage a quarter of the period, as FBD, using the time-variable τ as a mathematical ploy to get the unbiased voltage as a function of t, avoiding the constant term resulting from an indefinite integral. However, the difference in the mathematical procedure gives different results between FBD and CPT.

Let's suppose a system with voltage distortion and a negligibly DC level such that:

$$u(t) = \sqrt{2}\sum_{h=1}^{H} U_h \sin(h\omega_1 t + \alpha_h) \qquad (14)$$

Then, the unbiased integral of $u(t)$ would be:

$$\hat{u}(t) = \int_0^t u(\tau)(d\tau) = \sqrt{2}\sum_{h=1}^{H} -\frac{U_h}{h\omega_1}\cos(h\omega_1 t + \alpha_h) \quad (15)$$

Indeed, the voltage was displaced a quarter of the period. However, each harmonic component is divided by its frequency. This implies that the higher the harmonic order, the lower its impact on $\hat{u}(t)$. Even in a system without voltage distortion, $\hat{u}(t)$ is ω_1 times lower than $u(t)$. This filtering to displaced harmonic components matches the widely accepted criteria that reactive power is only defined for the fundamental frequency [20]. Fig. 4 shows the displaced and unbiased voltages calculated from a measure from a system implemented in the lab. The voltage signal at the PCC has a flat-top waveform, which is the typical waveform seen in distribution systems [21].

As mentioned, $u(t)$ and u_d (t) have the same waveform but displaced 1/4 of a period. Otherwise, $\hat{u}(t)$ is almost sinusoidal, confirming that unbiased integral tends to reduce the harmonic voltage components with a phase displacement.

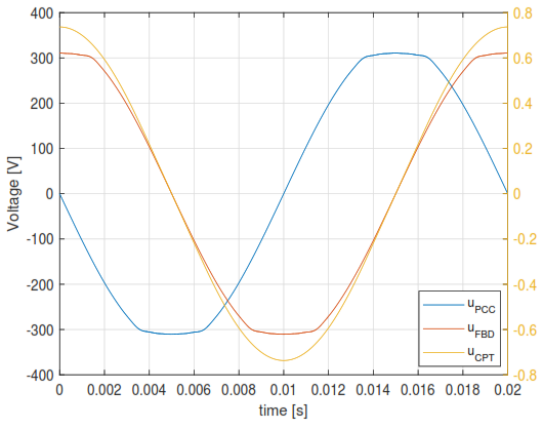

Figure 4. Displaced voltage (u_{FBD}) and unbiased voltage (u_{CPT}) were calculated from u_{PCC} measured. Note that u_{CPT} is 340 times smaller than the other voltages. Source: Own elaboration.

Nevertheless, from $\hat{u}(t)$ is calculated the quantity W related to the presence of reactive power in the system:

$$W = \frac{1}{T}\int_{\tau}^{\tau+T} i(t)\hat{u}(t)dt \quad (16)$$

which in turn defines the reactive current i_r similar to FBD.

$$i_r(t) = B\hat{u}(t) = \frac{W}{\hat{U}^2}\hat{u}(t) \quad (17)$$

Finally, the void current i_V (t) is defined as shown in Eq.18. This component is associated with current distortion non-related to voltage, meaning that no harmonic of i_V (t) should match the harmonics of $u(t)$.

$$i_V(t) = i(t) - i_a(t) - i_r(t) \quad (18)$$

An important advantage of this approach that shares with FBD is that W is a conservative quantity derived from a linear decomposition, which implies the accomplishment of Tellegen's Theorem [22], a generalization of Kirchhoff Laws. In addition, CPT clearly describes reactive power usage in the system.

3.3. Current's Physical Components Power Theory (CPC)

This power theory was developed from a hybrid time-domain and frequency-domain approach. The load depicted in Fig. 5 is modeled using the admittance Y in the frequency domain such that:

$$Y_h = G_h + jB_h \quad (19)$$

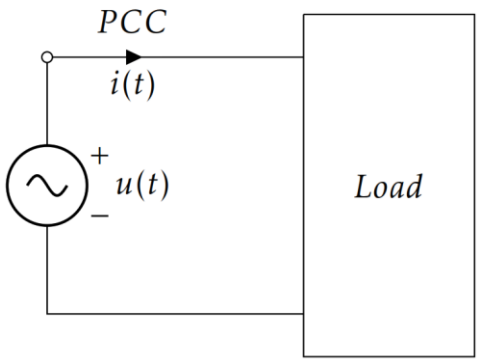

Figure 5. CPC Power theory. Source: Own elaboration.

Y_h is not a theoretical admittance and has to be measured, which implies an additional challenge for the measurement campaign and data processing. As the other power theories presented above, the active power is defined from the supposition of the conductance (G) presented in equation 8. In this way, the *active current* can be calculated as:

$$i_a(t) = Gu(t) = \sqrt{2}Re\sum_{h=1}^{H} GU_h e^{jhw_1 t} \quad (20)$$

Then, the non-active current is calculated as:

$$i(t) - i_a(t) = \sqrt{2}Re\sum_{h=1}^{H}(G_h + jB_h - G)U_h e^{jhw_1 t} \quad (21)$$

In turn, this quantity can be decomposed into two new currents called *reactive current* i_r and *scattered* current i_s:

$$i_r(t) = \sqrt{2}Re\sum_{h=1}^{H} jB_h U_h e^{jhw_1 t} \quad (22)$$

$$i_s(t) = \sqrt{2}Re\sum_{h=2}^{H}(G_h - G)U_h e^{jhw_1 t} \quad (23)$$

As the active current, these quantities can be rewritten as:

$$i_r(t) = \sqrt{2}\sum_{h=1}^{H} -B_h U_h sin(hw_1 t) \quad (24)$$

$$i_s(t) = \sqrt{2}\sum_{h=2}^{H}(G_h - G)U_h cos(hw_1 t) \quad (25)$$

Note that $i_r(t)$ contains phase displacement information in the frequency spectrum. On the other hand, $i_s(t)$ contains information related to harmonic components produced by the difference between a reference active power (calculated by means G) and the active harmonic components present in the system, represented by G_h. Despite CPC being well thought out in terms of circuit theory, the amount and quality of information needed for calculation could eventually lead to misinterpretations or mathematical errors; in other words, CPC application could not be pretty practical in real systems. A detailed process description is presented in [17].

4. Study Case and Comparison Between Power Theories

A microgrid was implemented in the Power Quality Laboratory of the Institute of Electric Power Systems and High Voltage Engineering (IEEH) of the TUD Dresden University of Technology, as shown in Fig. 6.

This system explores the advantages and disadvantages of the previously presented power theories. It is also used to test some methods of harmonic contribution assessment [23].

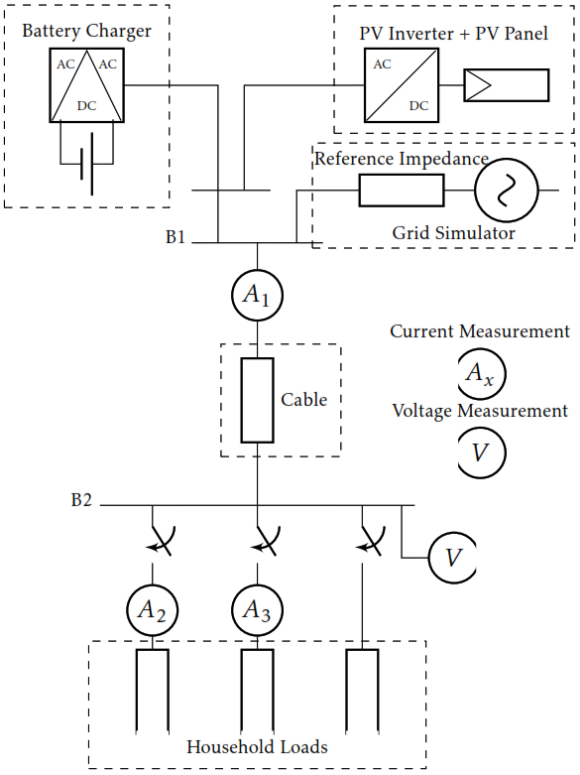

Figure 6. General scheme of the system implemented in Lab. Source: Own elaboration.

4.1.1. PV Inverter

The PV Inverter is an SMA Sunny Boy 5000TL. The characteristics of the PV are summarized in Table 1. This equipment is fed using a PV-Simulator, which can simulate the power generated by the solar panels. The PV-simulator can be programmed to give any desired active power [23].

4.1.2. Battery Converter

The Battery converter is an SMA Sunny Island. The technical characteristics of the device are summarized in Table 1. A programmable DC-voltage source was connected to the DC side of the battery converter instead of genuine batteries to guarantee a flexible operation during the measurements.

Table 1. Characteristics of the sources

	PV Inverter	Battery Converter
Manufacturer	SMA Solar Technology AG	SMA
Product name	Inverter Sunny Boy 5000TL	BatteryInverter Sunny Island
Model number	SB 5000TL-21	SI3.0M-11
$P_{out\text{-}nom}$	4600 W	2300 W
$S_{out\text{-}nom}$	5000 VA	
$U_{AC\text{-}nom}$	230 V	
$I_{out\text{-}nom}$	20 A	10 A
f	50/60 Hz	45-65 Hz

Source: Own elaboration.

4.1.3. Household Loads

Three types of household appliances with different electronic topologies were selected for the measurements: linear load (Linear), non-linear loads composed of single-phase switch mode power supplies with active power factor correction (APFC), and nonlinear loads without power factor corrector (NPFC). Only loads with a constant operating mode or that can be fixed to have a constant power demand were selected. Table 2 lists the household appliances and their rated powers.

Table 2. Characteristics of the household loads

Appliances	Available Devices	Topology and Rated Power per Device [W]		
		Linear	NPFC	APFC
Water heater	2	2000		
Desktop computer	2			100
Laptop	2		100	
Incandescent lamps	2	60		
CFL ≤25 W			400	
CFL > 25 W				100
Total Available Load		4120	600	300

Source: Own elaboration.

4.1.4. Measurement Device

The Dewetron 2600 with HIS-HV and HIS-LV modules was used for the measurements as shown in Fig. 6. The voltage is measured directly with the modules Dewe HIS-HV, and the currents are measured using zero-flux transducers connected to the Dewe HIS-LV modules. The ratio of the transducers is 1:600 with a maximum current of 60*A* and bandwidth of 800*kHz*. The voltage and the currents were measured for 10 s per load scenario at a sample rate of 1 MS/s following the procedure presented in subsection 4.2. The voltage uncertainty is in the range of [1% - 15%] ± 7 mV for [1 – 0.06 V] as the input range for the frequency range of interest. Similarly, for the current measurement, the uncertainty lies in the range of [1% - 15%] in magnitude and [0 – 20°] in phase angle for [1000 – 2 mA] as the input. More information on the measurement device can be found in [23].

4.2. Measurement Procedure

Two connection modes were tested: islanded (ISM) and interconnected (ICM). In ISM, the PV inverter and the battery converter supply power to the bus bar B1. In this mode, the battery converter operates as a voltage reference for the PV inverter. However, note that if the network impedance is much lower than the load impedance, the load can influence the voltage waveform. A complete analysis of the impact of harmonic impedance over voltage and current harmonics can be found in [23]. In ICM, the battery converter and the PV are disconnected, and a grid simulator feeds the loads. Finally, different combinations of loads were connected to different power generation. Table 3 summarizes the apparent powers of the performed tests. Note that the combination of loads emulates different harmonic pollution scenarios. The linear load is a non-polluting case, the non-power factor correction load (NPFC) represents the high pollution case, and the MIX load, composed of a combination of all appliances available, is an intermediate pollution scenario. Finally, active power factor correction load (APFC) represents a case where a compensation scheme is introduced in the system.

Table 3. Summary of apparent powers for each test

	ISM [VA]			ICM [VA]
	Battery	PV	Load	Bus bar
NPFC	599.94	535.29	794.70	1061.22
APFC	339.18	0.53	338.65	336.41
LIN	1030.62	1174.50	2204.84	2143.82
MIX	2128.11	1188.49	3257.11	3174.35

Source: Own elaboration.

4.3. Impedance Characteristic of the Load Scenarios

The impedance characteristic for each loading scenario was measured over node B2 using a discrete frequency sweep. Currents with frequencies close to the harmonics were injected into the system, and the resulting voltage and the currents injected were computed to calculate the impedance characteristic. A more detailed description of the process and an analysis of the harmonic impedance and its impact on harmonic emission on the microgrid implemented in Fig. 6 can be found in [23].

4.4. Results

4.4.1. RMS Values and Scale Factor

The four scenarios were performed, and the original quantities were scaled using as reference the RMS value of the total current measured over each element as follows. From equations presented in section 3.1, it is possible to say that:

$$\begin{aligned} i(t) &= i_a(t) + i_{qd}(t) + i_D(t) \\ i(t) &= i_a(t) + i_r(t) + i_V(t) \\ i(t) &= i_a(t) + i_r(t) + i_s(t) \end{aligned} \tag{26}$$

Given that FBD, CPT, and CPC currents are orthogonal quantities, 26 can be rewritten in terms of RMS values as:

$$\begin{aligned} I^2 &= I_a^2 + I_{qd}^2 + I_D^2 \\ I^2 &= I_a^2 + I_r^2 + i_V^2 \\ I^2 &= I_a^2 + I_r^2 + I_s^2 \end{aligned} \tag{27}$$

Then, the quantities derived from 27 represent the size of each current component depending on the total RMS current measured in the PCC. These quantities allow the comparison between the different load scenarios:

$$\begin{aligned} 1 &= \frac{I_a^2}{I^2} + \frac{I_{qd}^2}{I^2} + \frac{I_D^2}{I^2} \\ 1 &= \frac{I_a^2}{I^2} + \frac{I_r^2}{I^2} + i_V^2 I^2 \\ 1 &= \frac{I_a^2}{I^2} + \frac{I_r^2}{I^2} + \frac{I_s^2}{I^2} \end{aligned} \tag{28}$$

Note that equation 28 can also be used as an estimator of the error as follows:

$$e_{FBD} = \left| 1 - \frac{I_a^2}{I^2} + \frac{I_{qd}^2}{I^2} + \frac{I_D^2}{I^2} \right| \tag{29}$$

Table 4 shows the RMS scaled currents and errors calculated for each loading scenario in ISM and ICM.

The first thing worth mentioning is that the higher the distorted current in the system, the higher the error in the three power theories. This fact can be explained by noise in high harmonic pollution scenarios and numerical calculation issues. Errors for FBD and CPT are shallow, and FBD has the highest performance. On the other hand, errors in CPC make evident the issues associated with the information requirements for this power theory implementation, like impedance measurement itself and the impossibility of making such measurements simultaneously with the voltage and current, situations that could derive misleading conclusions.

Table 4. RMS values of the current components using the total current as the scale factor

Load	**NPFC**		**APFC**		**MIX**		**LINEAR**	
Source	**ICM**	**ISM**	**ICM**	**ISM**	**ICM**	**ISM**	**ICM**	**ISM**
U	228.525	233.791	229.738	230.815	217.452	226.854	221.317	227.790
I	4.602	3.391	1.460	1.103	13.837	14.088	9.328	9.560
I_a	2.855	2.640	1.400	0.982	13.446	13.771	9.326	9.560
I_a/I	0.385	0.606	0.920	0.792	0.944	0.956	1.000	1.000
I_{qd}/I	0.085	0.010	0.059	0.155	0.008	0.003	0.000	0.000
I_D/I	0.530	0.384	0.021	0.053	0.047	0.042	0.000	0.000
e_{FBD}	0.001%	0.000%	0.001%	0.004%	0.000%	0.000%	0.000%	0.000%
I_r/I	0.085	0.004	0.061	0.152	0.014	0.002	0.000	0.000
i_V/I	0.535	0.393	0.023	0.054	0.049	0.041	0.000	0.000
e_{CPT}	0.516%	0.235%	0.399%	0.197%	0.715%	0.206%	0.003%	0.001%
I_r/I	0.047	0.042	0.042	0.023	0.000	0.000	0.000	0.000
I_s/I	0.841	0.009	0.218	0.073	0.000	0.001	0.001	0.000
e_{CPC}	49.336%	60.200%	5.126%	1.603%	0.002%	0.027%	0.44%	0.56%

Source: Own elaboration.

Another important thing is that the FBD and CPT current components are very similar. As it was discussed in section 3, the difference between these two theories lies in the definition of phase displacement, actually, in the absence of voltage distortion $i_r = i_{qd}$ and $i_V = i_D$. On the other hand, in the absence of phase displacement, $i_r = i_{qd} = 0$ and $i_V = i_D$.

4.4.2. Linear Load Scenario

As is shown in Table 4, there is an agreement between the three power theories for the Linear load scenario. This is a trivial result given that active power is calculated similarly and an important presence of other power quality phenomena is not expected. Fig. 7 shows the current components associated with each power quality phenomenon analyzed using each theory. Once again, it is clear that, for definition, active current is an image of the voltage waveform, no matter the calculus method used, as it was explained in section 2. Figure 7 also shows the current components associated with phase displacement and distortion. Here are some remarks about it:

- Phase Displacement in ISM: The waveform is quite similar calculated by the three power theories and, in the absence of voltage distortion, can be considered a displaced image of the voltage waveform.
- Distortion in ISM: The signals follow a pattern. However, its magnitude is too small to be considered an issue, as shown in Table 4.
- Phase Displacement in ICM: FBD and CPC are higher than CPT, given the voltage distortion. Here, the definition of phase displacement for FBD and CPC includes all displaced harmonic components. Otherwise, CPT includes in the definition only the fundamental harmonic component.
- Distortion in ICM: In contrast with phase displacement, the void current of CPT is higher than the distorted current of FBD. This is due to void current containing all frequency components that do not have a voltage reference but also frequency components with a displaced voltage reference.

4.4.3. MIX Load

The load for this scenario is composed of the NPFC load (700 W), the linear load (2000 W), and the APFC load (300 W). Then, a high distortion is expected, given the 1 kW of non-linear load composition. However, as also seen in Table 2, linear appliances in the experiment constitute the main part of the MIX. Therefore, this scenario's distorted current (also void and scattered currents) is shallow compared to the total load, as seen in Table 4. Because of the load composition, in this scenario, the results are similar to the Linear load scenario. In this way, previous remarks can be extrapolated to this scenario.

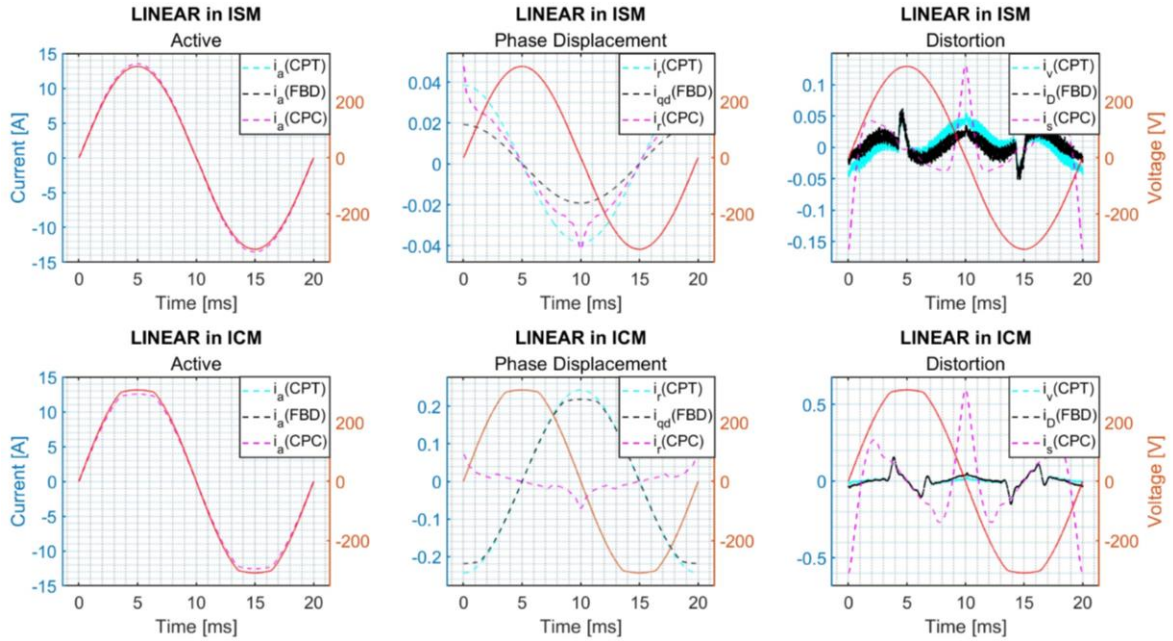

Figure 7. Current decomposition for the Linear scenario in both operation modes. The voltage was plotted in red as a visual reference.

4.4.4. Non-linear Load (NPFC)

From Table 4, it is possible to see that CPC results are unreliable in the presence of distortion. On the other hand, in Fig. 8, it is possible to see that FBD and CPT currents match very well, given that there is a low phase displacement compared to the total current.

4.4.5. Non-linear Load with compensation scheme (APFC)

The calculation results of this scenario are similar to the previous case. However, it could be interesting, both in this scenario and in the others, to analyze the changes in the current components according to the type of load and source, as will be seen in the next section.

5. Power Quality Phenomena Assessment From FBD and CPT Power Theories

Up to this point, it is clear that CPC has no reliable results in high-distortion scenarios. In addition, some issues associated with information acquisition, like the impossibility of making impedance measurements simultaneously with the voltage and current, can lead to wrong conclusions. On the other hand, FBD and CPT present similar (or even equal) results in some particular conditions, namely: 1. Low voltage distortion, 2. Low phase displacement. As was already mentioned, the difference lies in the phase displacement definition. FBD gives a broader description of this phenomenon, including the fundamental displaced component and all displaced harmonic currents. CPT excludes such displaced harmonic, approaching the reactive power definition. Figure 9 shows the scaled RMS value of I_{qd} and I_r. In all load scenarios, the current is almost the same. However, I_{qd} is slightly higher for the reasons previously exposed. The highest difference can be found in the NPFC load scenario, given that this has the higher distortion.

In traditional power systems, namely, those with a high short-circuit ratio, voltage distortion is not a problem compared with the distortion caused by some non-linear loads. In other words, If the short circuit ratio is high enough, the voltage waveform is stiff and not influenced by the load. This way, CPT or FBD could be indifferent, given that the results should be almost identical. However, in nontraditional power systems, like microgrids, the distortion caused by the loads can change the voltage waveform. As was already mentioned, the four load compositions implemented in the microgrid emulate different distortion conditions in the system.

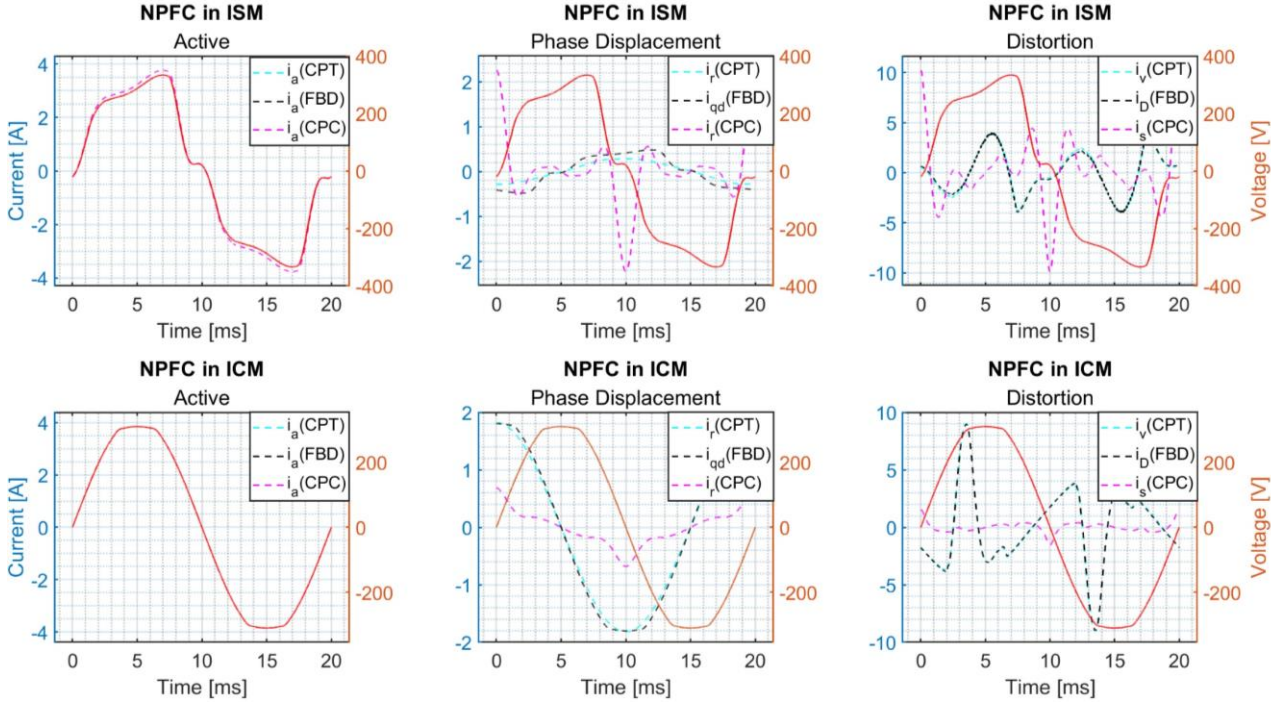

Figure 8. Current decomposition for NPFC scenario in both operation modes. The voltage was plotted in red as a visual reference.

In addition, the interconnection mode simulates the two possible scenarios in a system; ICM represents a robust network whose voltage waveform can hardly be disturbed by the load. In addition, the network has a characteristic voltage distortion, as shown in Fig. 7. Otherwise, ISM represents a weak network that the load can easily disturb. In addition, the inverter voltage output is usually a perfectly sinusoidal wave form (Fig. 7).

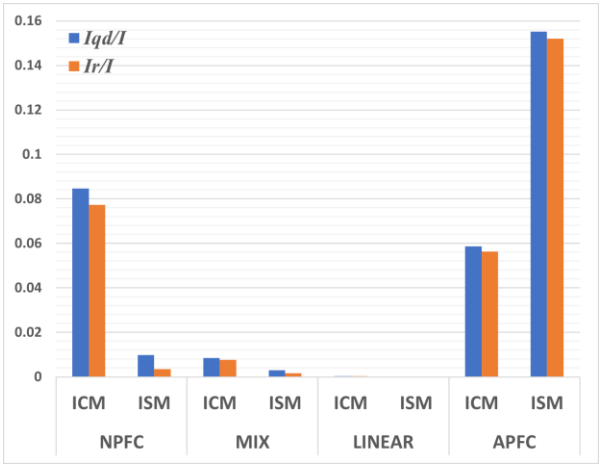

Figure 9. RMS scaled values of the current components I_{qd} and I_r calculated from CPT. Source: Own elaboration.

Figure 10 shows the RMS scaled values of I_a and I_D. In the linear load scenario, it is clear that almost all power delivered from source to load is active, even in the presence of voltage distortion (ICM), I_D is not an issue for the system. The same conclusion applies to the MIX load scenario; a distorted current is less than 5% of the total current. In addition, the difference in distortion between ICM and ISM is barely observable. In the NPFC load scenario, the situation is completely different. In ICM, there is a high distortion, and less than the 40% of the current delivered is active. However, it is worth highlighting two things:

- Given that the network is strong, and consequently, the load cannot modify the voltage waveform, it is possible to say that the load causes the distorted current.
- As mentioned, the active current contains the effect of voltage distortion. On the other hand, the active component can only flow from source to load. In this way, the source is responsible for the active current component, including the voltage distortion reflected on it.

These highlights give it the key to asses responsibilities in strong networks (traditional distribution systems), namely: *The network is responsible for the active distortion and the load is responsible for non-active distortion*. Table 5 shows the contribution of the network and the load to the total current measured in the PCC. I_D is the same value shown in Table 4. On the other hand, $I_{Background}$ is the non-fundamental active current extracted from i_a using a Fast Fourier Transform. In these cases, it is possible to say that the main contributor (or main responsible) is the load.

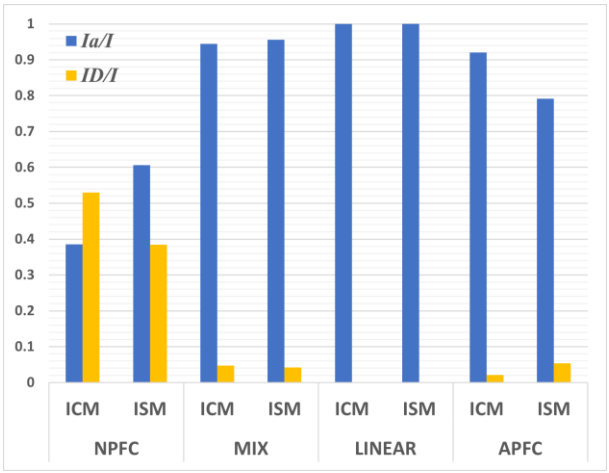

Figure 10. RMS scaled values of the current components I_a and I_D. Source: Own elaboration.

Table 5. Contribution of the Network ($I_{Background}$)and the load (I_D) to the Waveform Distortion in ICM

Type of Load	NPFC	APFC
$I_{Background}$	0.04%	0.09%
I_D	53.03%	2.11%

Source: Own elaboration.

This rule can be practical but valuable only in traditional networks. In ISM, there is a highly distorted current and an even higher active current that also contains voltage distortion, as seen in Fig. 8. However, as was already mentioned, the voltage waveform at the output of the inverter was a perfect sinusoid. This means the load has modified the voltage waveform, causing voltage distortion. Differences between FBD current components in ICM and ISM sum zero. This fact explains the increase in the active current compared to the ICM. In other words, a part of the distorted current is converted into the active current, more precisely in voltage distortion. Finally, it is possible to say that the load is responsible for the active and non-active distortion as long as the voltage waveform before the connection of the load is known. Table 6 shows the voltage distortion reflected on

I_a and the distorted current I_D in the percentage of the total current measured on the PCC. As mentioned, the load is responsible for these particular active and non-active distortion cases.

Table 6. Contribution of the Load to the Waveform Distortion in ISM

Type of Load	NPFC	APFC
$I_{Background}$	1.89%	0.09%
I_D	38.41%	5.31%

Source: Own elaboration.

6. Conclusions

In this paper, FBD, CPT, and CPC power theories were reviewed and tested in a system implemented in the laboratory. The decomposition of current that each of them proposes was used to assess waveform distortion contribution on the PCC, and some conclusions were derived from this exercise:

- The three power theories have a plausible mathematical development. However, the simplicity of FBD makes it easy to understand and implement. On the other hand, CPC is more complicated, and its implementation requires harmonic impedance measurement.
- An indicator to calculate errors in the power theories was applied. The results of FBD and CPT were acceptable, while CPC results were unreliable in this exercise, particularly in scenarios with high waveform distortion.
- The current components derived from CPT and FBD are almost the same. As mentioned, the main difference lies in the reactive (CPT) and displaced (FBD) current components. However, there are two conditions under which the current components of these power theories should be equal: Low voltage distortion in the network and low reactive power in the system.
- Two types of networks were defined: strong and weak. Assessing waveform distortion contribution in strong networks is trivial, considering that the network is responsible for voltage distortion in the PCC, and the load is responsible for distorted (or void) current. However, assessing contributions in weak networks is more complex and requires knowing the voltage waveform before the loading.
- Under a hypothetical scenario with high distortion (or even distortion levels over the regulatory limit) and the possibility of changing the connection mode between the interconnected and the islanded, a part of the distorted (void) current generated in interconnected mode turns into active current (voltage distortion) in islanded mode. This implies that the load could be responsible for the distorted (void) current and a part of the active current in weak networks.

Funding acquisition

This project is supported by DAAD with funds from the German Federal Ministry of Education and Research (Project ID: 57447921) and MinCiencias with funds from the National Fund for Science, Technology and Innovation, Francisco José de Caldas (Project ID: 64996).

Autor Contributions

C. Garzón: Conceptualization, Formal Analysis, Funding Acquisition, Investigation, Methodology, Software, Writing, Visualization. A. M. Blanco: Conceptualization, Funding Acquisition, Investigation, Methodology, Resources, Review & Editing, Project Administration, Validation. A. Pavas: Conceptualization, Funding Acquisition, Investigation, Supervision, Review & Editing, Validation. J. Meyer: Conceptualization, Funding Acquisition, Resources, Supervision, Review & Editing, Validation.

All authors have read an agreed to the published version of the manuscript.

Conflicts of Interest

The authors declare no conflict of interest.

Institutional Review Board Statement

Not applicable.

Informed Consent Statement

Not applicable.

References

[1] IEEE, “IEEE Recommended Practice and Requirements for Harmonic Control in Electric Power Systems,” IEEE Std 519-2014 (Revision of IEEE Std 519-1992), pp. 1–29, 2014, doi: https://doi.org/10.1109/IEEESTD.2014.6826459

[2] IEC, "Part 3-6: Limits - Assessment of emission limits for the connection of distorting installations to MV, HV and EHV power systems," Electromagnetic compatibility (EMC) - IEC TR Std. 61000-3-6, pp. 1–29, 2008. [Online]. Available: https://webstore.iec.ch/publication/4155

[3] A. Spelko, B. Blazic, I. Papič, M. Pourarab, J. Meyer, X. Xu, and S. Z. Djokic, "Cigre/cired jwg c4.42: Overview of common methods for assessment of harmonic contribution from customer installation," in *2017 IEEE Manchester PowerTech*, pp. pp. 1-6 , 2017, doi: https://doi.org/10.1109/PTC.2017.7981195

[4] T. Pfajfar and I. Papič, "Harmonic emission level estimation based on measurements at the point of evaluation," in *2011 IEEE Power and Energy Society General Meeting*, pp. 1–5, 2011, doi: https://doi.org/10.1109/PES.2011.6039642

[5] C. Garzón, A. Pavas, "Review of responsibilities assignment methods for harmonic emission," in *2019 IEEE Milan PowerTech*, pp. 1–6, 2019, doi: https://doi.org/10.1109/PTC.2019.8810742

[6] R. L. A. E. Emanuel. A. Testa, "Power definitions for circuits with nonlinear and unbalanced loads — the ieee standard 1459-2010," in *2012 IEEE Power and Energy Society General Meeting*, pp. 1–6, 2012, doi: https://doi.org/10.1109/PESGM.2012.6345330

[7] S. Fryze, "Effective reactive and apparent powers in circuits with nonsinusoidal waveforms," E*lectrotehn Zeitshrift*, vol. 53, pp. 596– 99, 1932.

[8] F. Buchhokz, "Understanding the correct power concept of active and reactive power," *Selbsverlag, Munchen*, 1950.

[9] IEEE, "Ieee standard definitions for the measurement of electric power quantities under sinusoidal, nonsinusoidal, balanced, or unbalanced conditions," IEEE Std 1459-2010 (Revision of IEEE Std 1459-2000), pp. 1–50, March 2010, doi: https://doi.org/10.1109/IEEESTD.2010.5439063

[10] L. S. Czarnecki, "What is wrong with the budeanu concept of reactive and distortion power and why it should be abandoned," *IEEE Transactions on Instrumentation and Measurement*, pp. 834–837, 1987, doi: https://doi.org/10.1109/TIM.1987.6312797

[11] A. Pavas, "Study of responsibilities assignment methods in power quality (summa cum laude)," Ph.D. dissertation, Universidad Nacional de Colombia, Facultad de Ingeniería, 2012.

[12] M. Depenbrock, "The FBD method, a generally applicable tool for analyzing power relations," *IEEE Transaction on Power Systems*, pp. 381 – 387, 1993, doi: https://doi.org/10.1109/59.260849

[13] A. Pavas, V. Staudt, H. Torres, "Method of disturbances interaction: Novel approach to assess responsibilities for steady state power quality disturbances among customers," *14th International Conference on Harmonics and Quality of Power (ICHQP)*, 2010, doi: https://doi.org/10.1109/ICHQP.2010.5625493

[14] P. M. P. Tenti, "A time-domain approach to power terms definitions under non-sinusoidal conditions," in 6th Int. Workshop on Power Definitions and Measurement under NonSinwwidal Conditions, Milan, Italy, 2003.

[15] P. M. P. Tenti, H. K. M. Paredes, "Conservative power theory, sequence components and accountability in smart grids," *2010 International School on Nonsinusoidal Currents and Compensation*, pp. 37–45, 2010, doi: https://doi.org/10.1109/ISNCC.2010.5524473

[16] L. S. Czarnecki, "Orthogonal decomposition of the currents in a 3-phase nonlinear asymmetrical circuit with a nonsinusoidal voltage source," in *IEEE Transactions on Instrumentation and Measurement*, pp. 30–34, 1988.

[17] L. S. Czarnecki, "Currents' physical components (CPC) concept: A fundamental of power theory," *2008 International School on Nonsinusoidal Currents and Compensation*, pp. 1–11, 2008, doi: https://doi.org/10.1109/ISNCC.2008.4627483

[18] C. Garzón, A. Pavas, "Laplacian eigenvector centrality as tool for assessing causality in power quality," *2017 IEEE Manchester PowerTech*, pp. 1–6, 2017, doi: https://doi.org/10.1109/PTC.2017.7981261

[19] A. Pavas, V. Staudt, and H. Torres, "Statistical analysis of power quality disturbances propagation by means of the method of disturbances interaction," *Conference on Innovative Smart Grids Technologies - Europe (ISGT-EU)*, 2012, doi: https://doi.org/10.1109/ISGTEurope.2012.6465817

[20] IEEE, "IEEE Standard Definitions for the Measurement of Electric Power Quantities Under Sinusoidal, Nonsinusoidal, Balanced, or Unbalanced Conditions," IEEE Std 1459-2010 (Revision of IEEE Std 1459-2000), pp. 1–50, 2010, doi: https://doi.org/10.1109/IEEESTD.2010.5439063

[21] S. Yanchenko, J. Meyer, "Harmonic emission of household devices in presence of typical voltage distortions," *2015 IEEE Eindhoven PowerTech*, pp. 1–6, 2015, doi: https://doi.org/10.1109/PTC.2015.7232518

[22] P. Penfield, R. Spence, S. Duinker, "A generalized form of tellegen's theorem," *IEEE Transactions on Circuit Theory*, vol. 17, no. 3, pp. 302-305, 1970, doi: https://doi.org/10.1109/TCT.1970.1083145

[23] S. Kannan, A. M. Blanco, C. Garzón, A. Pavas, and J. Meyer, "Harmonic impedance characteristics in an islanded microgrid and its impact on voltage and current harmonics," 2021 *IEEE Madrid PowerTech*, pp. 1–6, 2021, doi: https://doi.org/10.1109/PowerTech46648.2021.9494905